

## Determination of atmospheric turbidity at Pune

G R Aher & V V Agashe

Department of Physics, University of Poona, Pune 411 007

Received 27 May 1997; revised 26 August 1997; accepted 19 December 1997

Factors affecting atmospheric turbidity are discussed. The solar radiometer measurements carried out from Pune using narrow band interference filters are analysed to determine aerosol extinction coefficient, atmospheric turbidity coefficients and their monthly variations. Values of Angstrom turbidity coefficients  $\alpha$  and  $\beta$  are computed and the results are discussed. Coefficient  $\alpha$  which is correlated with aerosol size spectrum shows seasonal variation. For the visible region the mean value of  $\alpha$  is about  $-0.49$ , showing the dominance of large-sized aerosols. Angstrom turbidity coefficient  $\beta$  and Schuepp's turbidity coefficient  $B$  have a similar trend of variation with high values in summer and low values in winter. Angstrom turbidity coefficient  $\beta$  and Linke's turbidity factor  $T$  follow a linear relation. Their mean values for Pune lie in the ranges  $0.16-0.42$  and  $3.4-4.6$  respectively. Compared to the earlier reported study by Mani *et al.* [*Tellus (Sweden)*, 21 (1969) 829], summer turbidity at Pune has increased by 2.5-3 times. There is a rise in turbidity level at Pune even from 1986 to 1996, which is the period covered by the present study. The results show that atmospheric haze is a major contributor to the high turbidity value in February, while wind-blown dust and influx of aerosols through pre-monsoon circulation is a major source of high turbidity value during April-May.

### 1 Introduction

The intensity of solar radiation reaching the earth's surface is substantially modified by scattering and absorption in the atmosphere. When the solar radiation passes through the earth's atmosphere it suffers attenuation due to absorption and scattering by the gaseous constituents and by particulate matter. Depletion of solar energy in the direct solar beam is partly due to scattering by air molecules. When the scattering particles are small in comparison with the wavelength, Rayleigh scattering theory can be applied. In fact, Rayleigh theory is applicable when the radius of the scattering centre is less than  $0.1 \lambda$ . When  $r > 25 \lambda$ , geometrical optics may be used to compute the scattering effect. However, in the range  $0.1 \lambda < r < 25 \lambda$  one has to use more complicated theory developed by Mie.

Whereas atmospheric scattering is a continuous function of the wavelength, atmospheric absorption is in general selective. Ozone, which exists in the upper part of the stratosphere, absorbs chiefly in the ultraviolet, producing abrupt termination of solar radiation below 290 nm. In the

visible region, ozone has a weak absorption due to Chappuis bands (440-740 nm). Water vapour absorbs selectively in the infrared and has scattering properties as well. In the infrared, absorption by water vapour occurs at about 720 nm and above. Absorption by  $\text{CO}_2$  lies above 1600 nm.

In the visible region of the solar spectrum (400-750 nm), where gaseous absorption is minimal under clear sky conditions, aerosols are the major cause of depletion of direct solar radiation through scattering and absorption. The depletion is small in pure air but increases with the level of atmospheric turbidity associated with variable components in the air, such as water vapour, dust, haze or generally aerosol particles. The combined effect of scattering and absorption of solar radiation by aerosols is termed atmospheric turbidity. Measurement of direct solar radiation can be used to determine turbidity of the atmosphere. The authors operated a solar radiometer in the University of Poona to record the direct solar radiation at multiple wavelengths in the visible to near infrared region of the solar spectrum. These data are analysed to determine turbidity state of the atmosphere at Pune.

## 2 Experimental set up

Atmospheric extinction was determined by measuring spectral attenuation of direct solar radiation as a function of solar zenith angle. The solar radiometer consists of a long cylindrical cone having highly reflecting walls. The incident solar radiation first passes through optical interference filter and enters the reflecting cone channel. In the channel the filtered radiation gets scrambled due to multiple reflections from the walls of the cone and emerges as a homogeneous flux of monochromatic radiation. It is detected by the 'end-on' photomultiplier tube (PMT) placed at the exit end of the channel. The PMT output is proportional to the intensity of the transmitted flux of monochromatic radiation. Detailed description of the experimental set up is given elsewhere<sup>1,2</sup>.

The radiometer is directed at the solar disc with the help of a sighting telescope in which eyepiece is replaced by a ground glass screen. Field of view angle of the radiometer is kept small so as to collect light largely from the solar disc and exclude the neighbouring sky regions.

Observations were carried out from 0900 hrs till about 1700 hrs at 30-min intervals. The data consist of relative intensity of directly transmitted solar flux received at the ground as a function of solar zenith angle for selected wavelengths which are listed in Table 1. To eliminate the effect of clouds, measurements were made on clear days which occur at Pune generally from December to May. Atmospheric conditions thus become a controlling factor in the total period available for measurements and also in the daily observations. After subtracting the PMT dark current from the raw data, Langley plots were constructed whose slopes give the total extinction coefficient of the atmosphere, from which aerosol extinction coefficient was derived. In the present paper data for 1986-87, 1990-91 and 1996 are discussed.

## 3 Data analysis

For a parallel beam of monochromatic radiation,  $I_{0\lambda}$ , falling perpendicularly on a medium of layer of thickness  $l$ , the transmitted radiation  $I_\lambda$  is given by the Bouguer-Lambert relation

$$I_\lambda = I_{0\lambda} \exp(-a'_\lambda l) = I_{0\lambda} \exp(-a_{\lambda}) \dots (1)$$

where  $a'_\lambda$  is volume extinction coefficient with

Table 1—Optical wavelengths, Rayleigh extinction coefficients and ozone absorption coefficients

Wavelength nm	Rayleigh extinction coefficient	Ozone absorption coefficient, $\text{cm}^{-1}$
340	0.713	0.04
405	0.349	0
435	0.261	0
500	0.148	0.03
546	0.103	0.08
558	0.094	0.095
577	0.082	0.122
590	0.075	0.115
630	0.058	0.09
690	0.039	0.028
735	0.031	0.01
750	0.028	0.009

dimension  $L^{-1}$ . The product  $a'_\lambda l$  is called total extinction coefficient,  $a_{\lambda}$ , and is dimensionless. Since the solar radiation arrives at the earth's surface also at an inclined path, having longer path length,  $a_{\lambda}$  is multiplied by the optical air mass  $m$

$$I_\lambda = I_{0\lambda} \exp(-ma_{\lambda}) \dots (2)$$

where  $m = \sec Z$ ,  $Z$  being the zenith angle of the sun. In the logarithmic form, Eq (2) becomes

$$\ln I_\lambda = \ln I_{0\lambda} - a_{\lambda} \sec Z \dots (3)$$

Plot of  $\ln I_\lambda$  against  $\sec Z$ , known as Langley plot, is a straight line graph having negative slope,  $a_{\lambda}$ , which is total extinction coefficient of the atmosphere. The Y-intercept can be used for calibrating the solar radiometer. In the present study Langley plots having correlation better than 85% are included so that variance is estimated to be less than 2%. A typical Langley plot for the present data is shown in Fig. 1. It has a correlation coefficient of 0.976.

Molecular and particulate processes of scattering and absorption contribute to the total extinction coefficient. Therefore,  $a_{\lambda}$  may be expressed as the sum of extinction coefficients due to Rayleigh scattering  $a_{R\lambda}$ , gaseous absorption  $a_{g\lambda}$  and aerosol scattering  $a_{p\lambda}$ . Thus,

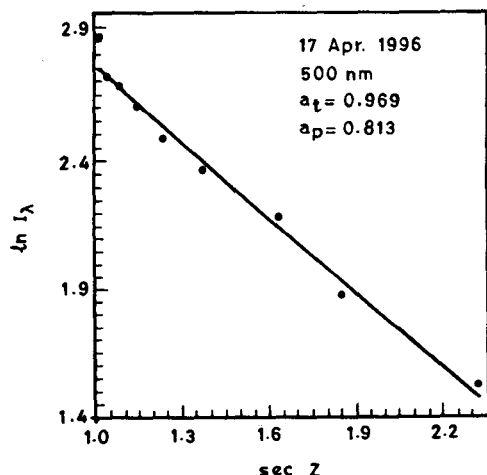


Fig. 1—A typical Langley plot showing collinearity of observed data points.

$$a_{i\lambda} = a_{R\lambda} + a_{g\lambda} + a_{p\lambda} \quad \dots (4)$$

For a model atmosphere at STP and for wavelength expressed in micron,  $a_{R\lambda}$  is given by Leckner's empirical relation (Eq. 5), which is reported to have only a small overall error<sup>3</sup>. The values are given in Table 1.

$$a_{R\lambda} = 0.008735 \lambda^{-4.08} \quad \dots (5)$$

In the visible region of the solar spectrum, only atmospheric ozone has a weak absorption<sup>3</sup> with absorption coefficient  $a_{o\lambda}$  (Table 1). If  $W_{oz}$  is the columnar content of atmospheric ozone (adopted from WMO-WODC values for Pune), the extinction coefficient due to gaseous (ozone) absorption can be written as,

$$a_{g\lambda} = W_{oz} a_{o\lambda} \quad \dots (6)$$

By substituting Eqs (5) and (6) in Eq. (4) aerosol extinction coefficient is derived. The derived  $a_{p\lambda}$  values are used in the calculation of atmospheric turbidity. The standard error in  $a_{p\lambda}$  is estimated to be less than 5%.

Several measures of turbidity are described in literature<sup>4</sup>. The most frequently used are Angstrom turbidity coefficients ( $\alpha$ ,  $\beta$ ), Schuepp's turbidity coefficient  $B$  and Linke's turbidity factor  $T$ . The relation between  $a_{p\lambda}$  and Angstrom's coefficients is given by Eq.(7) and that between  $B$  and turbidity coefficients by Eq.(8)

$$a_{p\lambda} = \beta \lambda^{-\alpha} \quad \dots (7)$$

$$B = 0.434 \beta 2^{\alpha} \quad \dots (8)$$

where wavelength  $\lambda$  is expressed in  $\mu\text{m}$ ,  $a_{p\lambda}$  is the integrated aerosol extinction coefficient,  $\beta$  is the extinction coefficient corresponding to  $1\mu\text{m}$  wavelength which depends on the concentration of aerosols in the atmosphere, and  $\alpha$  is related to the size distribution of aerosol particles. Large values of  $\alpha$  indicate a high ratio of small to large particles. The range of values which  $\alpha$  can take may lie between 4 and 0 or less (i.e. negative values). When the size of the aerosol particles is small, of the order of air molecules,  $\alpha$  should approach 4, and it should approach 0 (or become negative) for large-sized particles. A value of  $\alpha = 1.3 \pm 0.2$  is sometimes used in Eq. (7) as a reasonable average value to determine working value of  $\beta$  although Angstrom emphasized that  $\alpha$  should be determined as far as possible with  $\beta$  in every case<sup>5</sup>. This is facilitated by the use of linearized Angstrom equation given in Eq.(9)

$$\ln a_{p\lambda} = \ln \beta - \alpha \ln \lambda \quad \dots (9)$$

The Linke's turbidity factor  $T$ , which is related to the whole spectrum of solar radiation, equals the number of Rayleigh atmospheres required to produce the same extinction as the real atmosphere associated with  $T$ . It is given by

$$T = (\langle a_{p\lambda} \rangle / \langle a_{R\lambda} \rangle) + 1 \quad \dots (10)$$

where  $\langle a_{p\lambda} \rangle$  and  $\langle a_{R\lambda} \rangle$  are averages over the spectral region used. The corresponding wavelength happens to be  $0.546 \mu\text{m}$ , i.e. near the mean wavelength for the visible region.

#### 4 Results and discussion

Following the procedure described above, the daily solar flux measurements carried out during 1986-87, 1990-91 and 1996 were analysed to determine aerosol extinction coefficients from which turbidity coefficients were derived by linearizing the Angstrom equation [Eq. (7)] (Ref.6). To determine Angstrom coefficients, a graph of  $\log a_{p\lambda}$  vs  $\log \lambda$  is plotted (Fig. 2). Slope

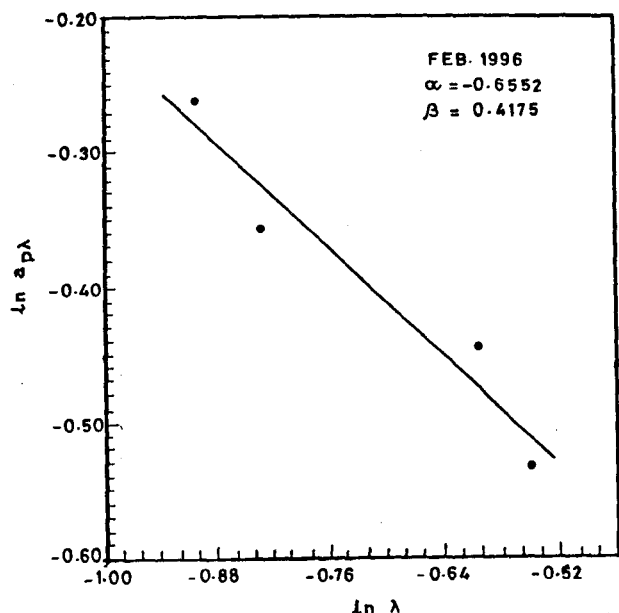


Fig. 2— $\ln a_{p\lambda}$  vs  $\ln \lambda$ .

of the straight line graph gives coefficient  $\alpha$  and intercept equals  $\ln \beta$  at  $1 \mu\text{m}$  wavelength. Thus both coefficients are determined simultaneously.

The Angstrom relation (Eq. 7) is empirical. Hence the plotted data may have some scatter. For the data presented in Fig. 2 correlation coefficient is around 0.99. With a high correlation coefficient, the derived  $\alpha$  and  $\beta$  values will not have large uncertainty. Although observations at larger number of wavelengths would be advantageous, the four or five wavelengths used in the present study are just sufficient to define the linear form of Angstrom relation.

4.1 Variation of Angstrom turbidity coefficient  $\alpha$

For comparing monthly variation of  $\alpha$  in different years the derived values are plotted (Fig. 3). The results show that  $\alpha$  is high in summer and hence small-sized particles dominate in this season. This shows that changes in aerosol size spectra can be studied from variation in  $\alpha$ . In this respect, values of  $\alpha$  during 1996 do not show any structure. The value of  $\alpha$  is about 1.0 in March 1987 and 1991, which again shows dominance of small-sized aerosol particles. It is negative for other months during these years, indicating a relatively high ratio of large to small particles.

The mean value of  $\alpha$  ranges between  $-0.4$  and  $-0.59$  during 1986-87, 1990-91 and 1996, showing

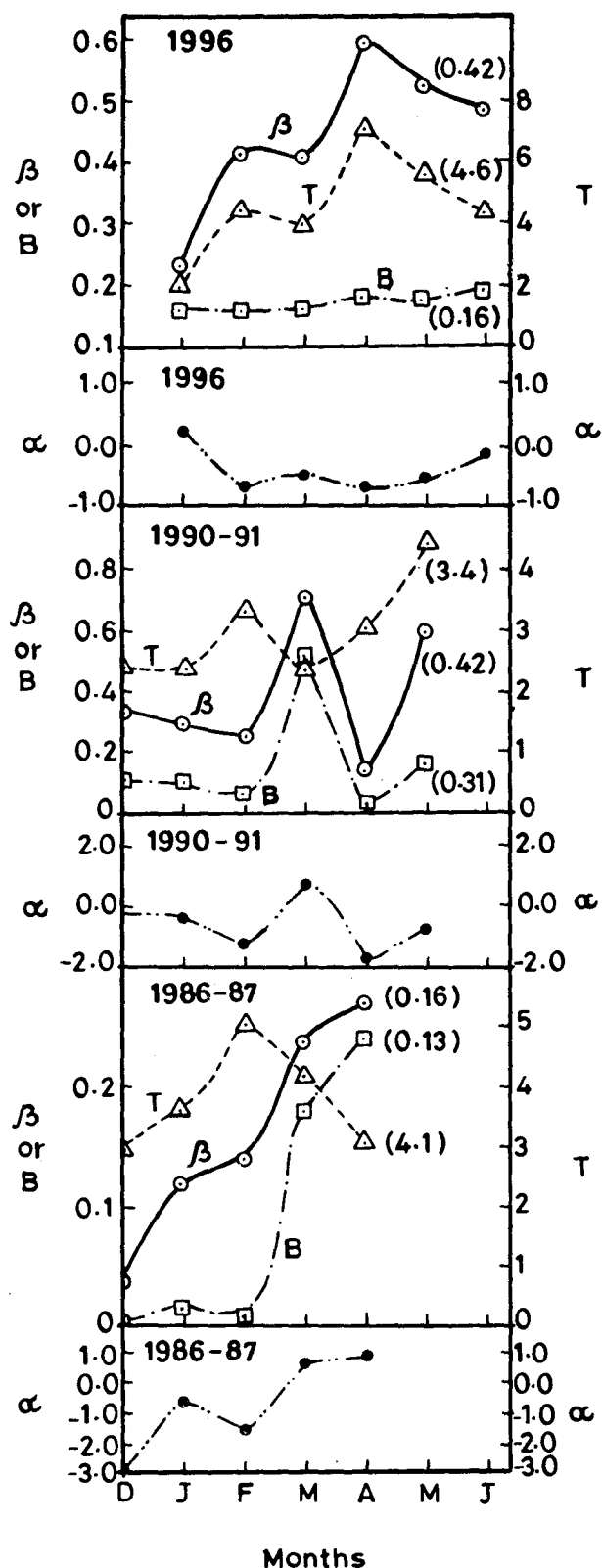


Fig. 3—Comparison of monthly variation of four turbidity coefficients (— $\Delta$ — $\Delta$ —  $T$ , — $\odot$ — $\odot$ —  $\beta$ , — $\square$ — $\square$ —  $B$ , — $\bullet$ — $\bullet$ —  $\alpha$ ; quantities in brackets are the seasonal averages).

a higher content of anthropogenic aerosols. In general, the values are positive as well as negative in a given observational season. This is seen in the results for 1986-87 and 1990-91, while during 1996 the values of  $\alpha$  are mostly negative.

Mani *et al.*<sup>5</sup> have reported a similar study carried out at Pune with a pyroheliometer and OG<sub>1</sub>, RG<sub>2</sub> and RG<sub>8</sub> filters during October 1968 to May 1969. They found that  $\alpha$  has a mean value of about 1.0 and remained more or less constant throughout the year. Comparing their results with the present results, it is seen that March 1987 and 1991 yielded the same value of  $\alpha$ . However in other months aerosol composition shows a considerable change. In 1968-69 aerosols consisted of small particles, whereas in 1996 they are composed of large-sized particles.

**4.2 Monthly variation of Angstrom and Schuepp's turbidity coefficients**

The monthly variation of  $\beta$  and  $B$  obtained by linear fitting method is shown in Fig. 3. The seasonal averages, given in brackets, are seen to increase in subsequent years, showing a rise in turbidity level from 1986 to 1996. In the monthly variation, turbidity is low in winter (Dec.-Jan.) and high in February and in summer. A high value of turbidity in summer is a global phenomenon<sup>5,7</sup>. It is due to wind-driven dust in lower atmosphere and its transport to higher levels by convection and turbulence. For the tropical station Pune, it may also indicate an influx of aerosols due to pre-monsoon circulation. Low turbidity in winter, also a global feature, is caused by diminished aerosol input due to colder ground surface and low surface winds.

In Eq. (8),  $\beta$  is essentially the aerosol scattering coefficient relative to the base e at  $\lambda = 1 \mu\text{m}$ , while  $B$  is the same relative to the base 10 for  $\lambda = 0.5 \mu\text{m}$ . The trend of the monthly variation of  $\beta$  and  $B$  is similar, as seen in the plots for 1986-87 and 1990-91. In accordance with Eq.(8), although  $B$  depends on  $\alpha$  and  $\beta$ , influence of the latter is more than that

of the former. If two pairs of corresponding  $\alpha$  and  $\beta$  values are selected (Table 2) such that in pair (1)  $\alpha$  is nearly equal while  $\beta$  has different values, and in pair (2)  $\beta$  is nearly equal while  $\alpha$  has different values, and  $B$  is computed in both the cases using Eq.(8), then it is found that when the values of  $\beta$  are different the calculated  $B$  values are different and when the values of  $\beta$  are nearly same  $B$  values are closer although  $\alpha$  values are different (Table 2). Thus, the calculated values of  $B$  follow the trend of  $\beta$  values. Therefore, lack of similarity in their monthly variation during 1996 is rather unexpected. The reason for this may be the absence of structure in the monthly variation of  $\alpha$  (Fig.3) which may indicate absence of seasonal variation in the aerosol size spectrum during 1996.

**4.3 Monthly variation of Linke's turbidity factor**

Figure 3 also shows the monthly variation of Linke's turbidity factor,  $T$ . Trend of monthly variation of  $T$  during different periods exhibits some similarities on year to year basis. The winter minimum and the summer maximum are the normal trends observed at Pune. There is a secondary peak in  $T$  in February which may be due to the precipitation of atmospheric moisture on cold mornings. Turbidity depends on the conditions in the first few kilometres of the atmosphere and the dispersal of haze from ground to higher levels. At the time of experimental measurements, atmospheric haze used to be relatively prominent on cold mornings. Analysis showed that February high in  $T$  could be due to weaker convection during forenoon period leading to mass loading of haze particles. This appears to be the special characteristics of the observing station<sup>1,2</sup>, i.e. Pune.

Many observers have reported correlation between turbidity parameters and the amount of precipitable water in the atmosphere<sup>8</sup>. To study this aspect,  $\alpha_{p,\lambda}$  values obtained from 1986-87 data were analysed and monthly average values of  $T$  were derived. To estimate the amount of precipitable water vapour in the local atmosphere, monthly average values of relative humidity (RH) were used in Leckner relation<sup>9</sup> given below, in which  $\theta$  is the ambient temperature in K.

$$w = 0.493 \text{ RH exp } (26.23 - 5416/\theta) \theta^{-1} \dots (11)$$

Daily weather charts published by IMD, Pune, contain data on dew point and surface temperature

Table 2—Influence of  $\alpha$  and  $\beta$  on  $B$

Pair No.	$\alpha$	$\beta$	$B$
1	-1.36	0.1361	0.0230
	-1.23	0.2450	0.0454
2	0.23	0.4175	0.1151
	-0.66	0.4116	0.1293

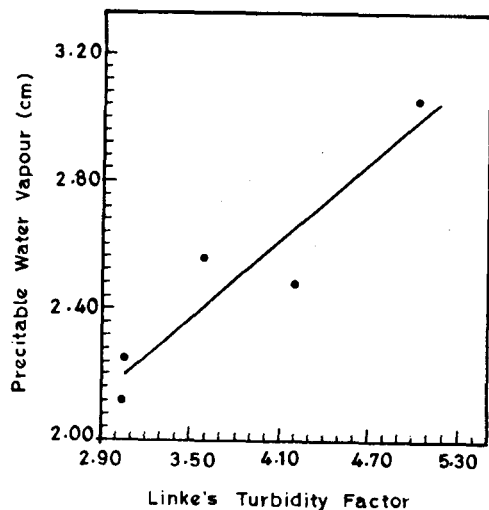


Fig. 4— $w$  vs  $T$ .

for various observing stations. For Pune, these data are given twice daily, once in the morning (M) at 0830 hrs, and the other in the evening (E) at 1730 hrs. These data were used for calculating monthly average values of RH. It has been found that for Pune, in general,  $[RH(M)] > [RH(E)]$ . Since precipitable water vapour will affect  $T$  through atmospheric haze, which is more likely to be present in the morning,  $[RH(M)]$  appeared a more likely candidate to study correlation with  $T$ . Precipitable moisture ( $w$ ) was calculated corresponding to daily morning  $[RH(M)]$  and monthly average  $w$  was derived. A plot of  $w$  vs  $T$  (Fig. 4) is found to be a straight line giving a correlation coefficient of 0.93.

#### 4.4 Relation between $\beta$ and $T$

In accordance with Eqs (7) and (10), the following relationship exists between  $\beta$  and  $T$ :

$$T = (\langle a_{p\lambda} \rangle / \langle a_{R\lambda} \rangle) + 1 = (\beta \lambda^{-\alpha} / \langle a_{R\lambda} \rangle) + 1 \quad \dots (12)$$

Substituting  $\langle a_{R\lambda} \rangle$  from Eq. (5) and the mean value of  $\alpha = -0.49$ , for the visible spectral range ( $\lambda = 0.546 \mu\text{m}$ ), Eq. (12) becomes

$$\begin{aligned} T &= (\beta \lambda^{4.57} / 0.008735) + 1 = 114.48 \beta (0.06295) + 1 \\ &= 7.2062 \beta + 1 \end{aligned}$$

or

$$\beta = -0.1388 + 0.1388 T \quad \dots (13)$$

The computed coefficients, more or less, satisfy

the linear relationship of Eq. (13). Combining Eq. (13) with Linke's statement that  $T = 3$  to 3.5 for pure country air, a fairly clean atmosphere<sup>4</sup> is associated with  $\beta$  between 0.088 and 0.11. For comparison, the present study gives overall average  $T$  between 3.4 and 4.6 and  $\beta$  between 0.16 and 0.42.

## 5 Conclusions

Intensity measurements of direct solar radiation at multiple wavelengths facilitate study of atmospheric turbidity. The analysis of radiometer data at Pune shows that Angstrom coefficient  $\alpha$  is high in summer, indicating predominance of small-sized aerosols and a seasonal change occurring in aerosol size spectra. It is more negative in the month of February, indicating the presence of large-sized aerosols with consequent rise in atmospheric turbidity which is indicated by the high value of  $T$  in February. This high value of  $T$  shows strong correlation with precipitable moisture in the atmosphere. This is coupled with low value of  $\beta$ . This may imply that the precipitable moisture has contributed to the growth in size of aerosols. From Eq. (8) it is seen that  $B$  is a function of both  $\alpha$  and  $\beta$ . Changes in aerosol size spectra are reflected in the monthly variation of  $B$ . However, the analysis shows that  $B$  is influenced more by  $\beta$ .

$T$ ,  $\beta$  and  $B$  have low values in winter and high values in summer. Low values of these coefficients in winter may be due to washout of aerosols after monsoon and reduced generation of aerosols. On the other hand, high value in summer may indicate seasonal influx of aerosols due to pre-monsoon circulation, wind-driven dust in the lower atmosphere and its transport to higher levels by convection and turbulence.

Mani *et al*<sup>5</sup> found that  $\beta$  shows strong seasonal variation, with maximum value of 0.23 in May and minimum value of 0.08 during November. The present measurements show that compared to earlier study by Mani *et al*.<sup>5</sup>, summer value of atmospheric turbidity at Pune has increased by 2.5 to 3 times.

From the definitions of the four coefficients discussed in this paper, while  $\alpha$  is related to the size distribution of aerosols,  $\beta$ ,  $B$  and  $T$  represent aerosol extinction.  $\beta$  and  $B$  represent aerosol

scattering at 1.0  $\mu\text{m}$  and 0.5  $\mu\text{m}$  respectively,  $T$  is closer to the total extinction. Thus, each coefficient has its own significance in describing the turbidity state of the atmosphere.

#### Acknowledgements

Aerosol studies at the University of Poona have been supported by grants from ISRO under the National Committee for Middle Atmosphere (NC-MA) and ISRO-GBP, from UGC under UGC-IMAP programme, and CSIR under Emeritus Scientist project. The authors thank the Head of the Physics Department and the University authorities for their encouragement.

#### References

- 1 Aher G R & Agashe V V, *Indian J Radio & Space Phys*, 25 (1996)197.
- 2 Aher G R & Agashe V V, *Bull Indian Aerosol Sci & Tech Assoc*, 8 (1995)32.
- 3 Iqbal M, *An Introduction to Solar Radiation* (Academic Press, New York), 1983, 115 and 127.
- 4 Nagel M R, *Appl Opt (USA)*, 14 (1975) 67.
- 5 Mani A, Chacko O & Hariharan S, *Tellus* (Sweden), 21 (1969) 829.
- 6 Cachorro V E, de Frutos A M & Casanosa J L, *Appl Opt (USA)*, 26 (1987) 3069.
- 7 Szymber R T & Sellers W D, *J Clim & Appl Meteorol (USA)*, 24 (1985) 725
- 8 Iqbal M, *An Introduction to Solar Radiation* (Academic Press, New York), 1983, 94.
- 9 Garrison J D & Adler G P, *Sol Energy (USA)*, 44 (1990) 225.